American Journal of Pathology, Vol. 154, No. 6, June 1999

Analysis of Intracytoplasmic Hyaline Bodies in a Hepatocellular Carcinoma

Demonstration of p62 as Major Constituent

Cornelia Stumptner,* Hans Heid,† Andrea Fuchsbichler,* Hubert Hauser,‡ Hans-Jörg Mischinger,‡ Kurt Zatloukal,* and Helmut Denk*

From the Departments of Pathology and Surgery,‡ University of Graz School of Medicine, Graz, Austria, and the Division of Cell Biology,† German Cancer Research Center, Heidelberg, Germany*

Intracytoplasmic hyaline bodies (IHBs) resemble inclusions in hepatocellular carcinoma cells, which so far have escaped further characterization. A relationship to Mallory bodies was suggested on the basis of light microscopy and filamentous ultrastructure. A hepatocellular carcinoma containing numerous IHBs was studied. Our studies revealed immunoreactivity of IHBs with the monoclonal antibodies SMI 31 and MPM-2, which recognize hyperphosphorylated epitopes present on paired helical filaments in Alzheimer's disease brains (SMI 31) or on diverse proteins hyperphosphorylated by mitotic kinases in the M-phase of the cell cycle (MPM-2). One- and two-dimensional gel electrophoresis of tumor extracts followed by immunoblotting with SMI 31 and MPM-2 antibodies revealed a major immunoreactive protein with an apparent molecular weight between 62 and 65 kd, which was resolved into several highly acidic (pH 4.5) protein components in two-dimensional gels. This protein was undetectable in non-neoplastic liver tissue. Sequence analysis identified the SMI 31 and MPM-2 immunoreactive material as p62, indicating that p62 is a major constituent of IHBs. p62 is an only recently discovered protein that is a phosphotyrosine-independent ligand of the SH2 domain of $p56^{lck}$, a member of the c-src family of cytoplasmic kinases. Moreover, p62 binds ubiquitin and may act as an adapter linking ubiquitinated species to other proteins. These features suggest a role of p62 in signal transduction and possibly also carcinogenesis. IHBs observed in the hepatocellular carcinoma cells presented are the first indications of a role of p62 in disease. ***(Am J Pathol 1999, 154:1701–1710)***

Different types of intracytoplasmic inclusions, such as hyaline bodies, pale bodies, α_1-antitrypsin (AAT)-containing globules, and Mallory bodies (MBs), have been found in hepatocellular carcinoma (HCC) cells.[1–11] MBs are complex filamentous protein aggregates that are associated with a variety of chronic liver disorders, particularly alcoholic and non-alcoholic steatohepatitis, but also benign and malignant hepatocellular neoplasms in man and experimental animals (for review see Ref. 12). They consist of cytokeratins (CKs) but also contain non-CK components[12–16] that are post-translationally modified, eg, by phosphorylation, partial proteolysis, and cross-linking.[17] AAT globules are present in some HCCs, not necessarily associated with AAT deficiency, and resemble abnormal cytoplasmic accumulations of this antiprotease.[11] Pale bodies usually contain fibrinogen.[6,11] In contrast, the nature of intracytoplasmic hyaline bodies (IHBs), which are not restricted to HCC cells,[2] is still controversial. IHBs are round or ovoid, ranging from barely visible globules to large inclusions. They are eosinophilic in hematoxylin and eosin (H&E) and red or blue in chromotrope aniline blue (CAB)-stained sections and remain unstained with the periodic acid-Schiff (PAS) reagent.[4,11] In electron microscopy, they present as a mixture of filamentous and granular material.[4] They do not react with antibodies to AAT, α1-fetoprotein, or CKs.[4] On the basis of their light and electron microscopic appearance, IHBs were thought to be related to, but not identical with, MBs.[1,4]

In the present communication we report immunohistochemical, ultrastructural, and biochemical analyses of IHBs and demonstrate p62, a recently described cytosolic protein playing a role in cellular signal transduction,[18,19] as a major constituent.

Case Report

A 62-year-old Caucasian male patient with liver cirrhosis, ascites, cholecystolithiasis, and a mass in the left lobe of the liver was admitted to the hospital. Liver biopsy revealed a well to moderately well differentiated HCC. The

Supported in part by Fonds zur Förderung der wissenschaftlichen Forschung (grant 7628-MED to H. Denk; grant S7401-MOB to K. Zatloukal).

Accepted for publication March 6, 1999.

Address reprint requests to Dr. H. Denk, Department of Pathology, University of Graz School of Medicine, Auenbruggerplatz 25, A-8036 Graz, Austria. E-mail: helmut.denk@kfunigraz.ac.at.

patient underwent lateral segment (segments 2 and 3) resection, which was initially well tolerated. The tumor was associated with a cirrhotic liver and measured ~7 cm in diameter. It was well delineated against the surrounding non-neoplastic tissue, although not encapsulated. Postoperatively, the patient's condition deteriorated, and progressively signs of liver failure developed. Despite intensive-care therapy, the patient died 20 days after the operation.

Material and Methods

Specimens of the surgically removed tumor and surrounding non-neoplastic liver tissue were fixed in phosphate-buffered (pH 7.4) 10% formaldehyde solution and conventionally embedded in paraffin. After removal of paraffin with xylene and rehydration, sections (4 μm thick) were stained with H&E, Perls iron stain, CAB, and PAS reagent with and without diastase digestion, respectively. Fixed and paraffin-embedded material was also used for immunohistochemistry. In addition, tissue was snap-frozen in isopentane precooled with liquid nitrogen immediately after resection and stored in liquid nitrogen for electrophoretic analysis, Western blotting, immunofluorescence, and electron microscopy.

Immunohistochemistry and Electron Microscopy

For indirect immunofluorescence microscopy, the following antibodies were applied to cryostat sections (3 μm thick, fixed in acetone at −20°C). Primary antibodies were M_M120-1 (specific for MBs[13]), SMI 31 (detecting an abnormally phosphorylated epitope on tau protein in paired helical filaments in Alzheimer's disease and hyperphosphorylated neurofilaments; Sternberger Monoclonals, Baltimore, MD), RT 97 (detecting paired helical filament-associated tau; Boehringer Mannheim, Mannheim, Germany[20]), SMI 34 (detecting phosphorylated neurofilaments; Sternberger Monoclonals), MPM-2 (detecting mitotic phosphoproteins; Upstate Biochemicals, Lake Placid, NY), R 27 (anti-lamin A+C[21]), X 223 (anti-lamin B2[21]), C219 (detecting MDR 1+3; Signet, Dedham, MA), tau-1 (Boehringer Mannheim), antibodies to phosphoserine (Sigma Chemical Co., St. Louis, MO), phosphothreonine (Sigma), phosphotyrosine (Sigma), tau (Sigma), neurofilament (Dako, Glostrup, Denmark), HBs antigen (Dako), CK 7 (OVTL 12/30; Monosan, Am Uden, The Netherlands), CK 8 (Ks 8.7; Progen, Heidelberg, Germany), CK 18 (Ks 18.04; Progen), CK 19 (Amersham, Little Chalfont, UK), CKs 8 and 18 (CK8/18; 50K160; produced in our laboratory[14]), HSP 60 (Stress Gene Biotechnologies Corp., Victoria, BC, Canada), HSP 70 (Santa Cruz Biotechnology, Santa Cruz, CA), HSP 90 (Transduction Laboratories, Lexington, KY), α1-fetoprotein (Dako), α1-antitrypsin (Dako), α1-antichymotrypsin (Dako), albumin (Dako), ubiquitin (Cambridge Research Biochemicals, Cambridge, UK; Chemicon International, Temecula, CA; Dako), αB-crystallin (Novocastra, Newcastle upon Tyne, UK), β-amyloid (Chemicon), fibrinogen (Dako), and 14-3-3 protein (Upstate Biochemicals). Secondary antibodies were tetramethylrhodamine (TRITC)-conjugated goat anti-mouse (Dianova, Hamburg, Germany) or fluorescein (DTAF)-conjugated swine anti-rabbit immunoglobulins (Dako). Controls with corresponding isotype immunoglobulins (Dako) were invariably negative. Double-immunofluorescence staining was performed as described previously.[13] Immunofluorescent specimens were analyzed with a MRC600 (BioRad, Richmond, CA) laser-scanning confocal device attached to a Zeiss Axiophot microscope. Different excitation wavelengths (488 nm for DTAF, 568 nm for TRITC, and a krypton/argon ion laser) were used.

Immunohistochemistry on paraffin-embedded tissue was performed with SMI 31 (dilution, 1:2000), MPM-2 (1:1000), and ubiquitin antibody (1:1000), respectively. The 4-μm-thick paraffin sections of formaldehyde-fixed material were deparaffinized, rehydrated, and either digested with 0.1% protease (type XXIV; Sigma) in PBS for 10 minutes (for SMI 31 and MPM-2) or microwaved in 0.1 mol/L citrate buffer, pH 6.0, at 750 W for 10 minutes (for demonstration of ubiquitin). Endogenous peroxidase was blocked by incubation in 1% H_2O_2 in methanol for 10 minutes. Incubation with primary antibodies for 1 hour at room temperature was followed by washing and incubation with biotinylated multi-link swine anti-goat, -mouse, and -rabbit Ig (Dako; dilution, 1:100) as secondary antibody and finally with the ABC complex using diaminobenzidine as chromogen (Dako).

For electron microscopy, 4-μm-thick frozen sections were fixed for 30 minutes in 4% paraformaldehyde (in PBS), dehydrated and resin (AGAR-100, Agar Scientific, Essex, UK) embedded. The 50-nm-thick sections were contrasted with uranyl acetate/lead citrate and studied with a Philips CM 100 electron microscope.

Gel Electrophoresis and Immunoblotting

Proteins were extracted from tumor and peritumor non-neoplastic liver tissue by sequential homogenization (followed by centrifugation) in low- and high-salt buffers containing 50 μg/ml leupeptin, 0.3 μmol/L aprotinin, 200 μmol/L Pefabloc SC, 1.0 μmol/L pepstatin, 2 mg/ml sodium fluoride, 0.1 mmol/L sodium pyrophosphate, and 0.2 mmol/L sodium vanadate to inhibit proteolysis. Briefly, frozen liver tissue (1.5 g) was homogenized (5% w/v) in low-salt buffer (LS; 90 mmol/L NaCl, 8 mmol/L KH_2PO_4, 5.6 mmol/L Na_2HPO_4, 0.5 mmol/L KCl, 10 mmol/L sodium EDTA, pH 7.4) using an Ultraturrax and centrifuged for 20 minutes at 10,000 × *g* at 4°C. The resulting pellet was rehomogenized in 30 ml of high-salt buffer (HS; 2 mmol/L KCl, 200 mmol/L NaCl, 10 mmol/L TrisHCl, pH 7.4) by 30 strokes in a Potter homogenizer, incubated on ice for 30 minutes, and centrifuged for 20 minutes at 10,000 × *g* at 4°C. The pellet was then resuspended in 30 ml of high-salt buffer containing 1% Triton X-100 (HSTX) and incubated on ice for 30 minutes followed by centrifugation at 10,000 × *g* for 20 minutes. The supernatants, ie, low-salt supernatant (LS-S), high-salt supernatant (HS-S), and high-salt/Triton X-100 supernatant (HSTX-S), were subjected to protein precipitation (1:1) with methanol/chloro-

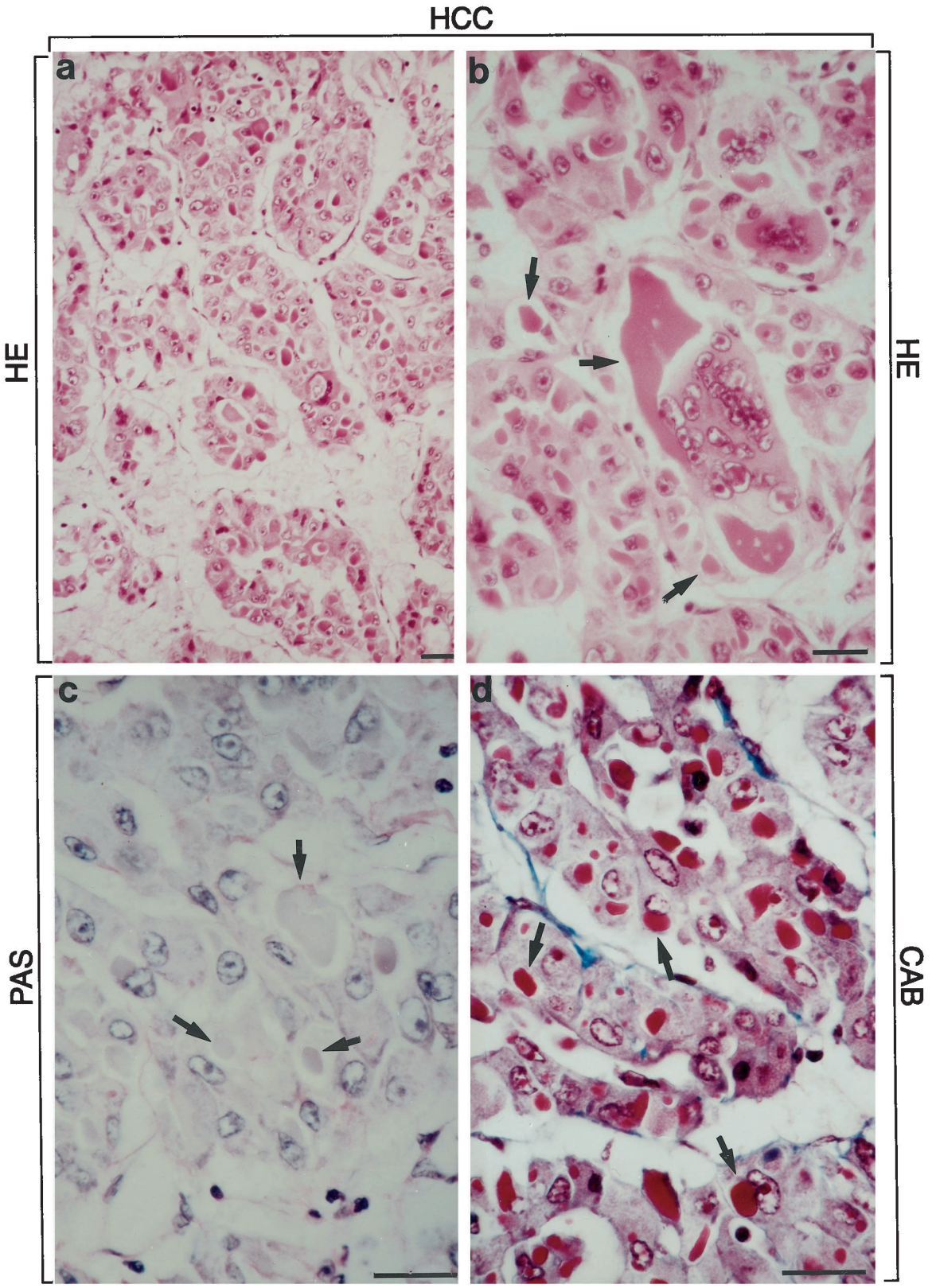

Figure 1. HCC with tumor cells arranged in trabecular and tubular (pseudoglandular) pattern. Numerous IHBs are present in tumor cells. IHBs are globular dense inclusions of different sizes surrounded by a clear halo. They stain eosinophilic in H&E-(a and b; arrows in b) and red (occasionally blue) in CAB-stained sections (arrows in d). They are PAS-negative (arrows in c). Multinuclear giant cell with large inclusion body is shown in b (arrows). Bars, 40 μm.

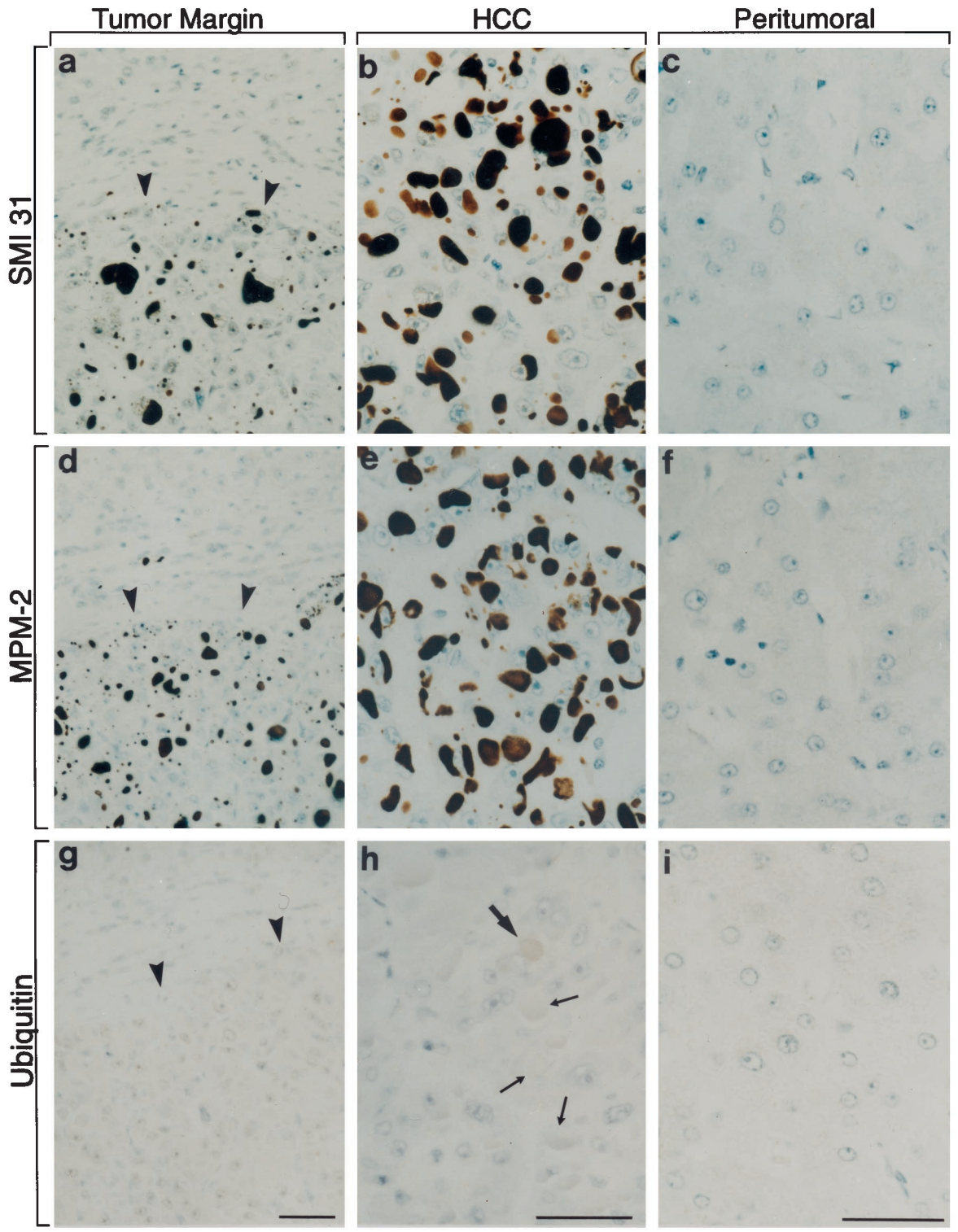

Figure 2. Immunohistochemical staining of HCC (a, b, d, e, g, and h) and peritumor (a, c, d, f, g, and i) non-neoplastic (cirrhotic) liver (border between HCC and peritumor liver indicated by arrowheads in a, d, and g) using monoclonal SMI 31 and MPM-2 antibodies as well as polyclonal antibodies to ubiquitin (ABC method). IHBs in tumor cells are stained with SMI 31 (a and b) and MPM-2 (d and e) whereas the surrounding non-neoplastic liver remains unstained. Some IHBs display a very faint staining with ubiquitin antibodies (thick arrow in h), but most remain unstained (thin arrows in h). Bars, 20 μm.

form (4:1). The high-salt-Triton X-100 protein pellet (HSTX-P) and the methanol/chloroform precipitated proteins were taken up in sample buffer and electrophoresed on 10% SDS-polyacrylamide gel.[14] For two-dimensional analysis, frozen tumor material was homogenized in sample buffer (9 mol/L urea, 35 mmol/L Trizma base, 65 mmol/L dithiothreitol (DTT), 4% CHAPS) using Eppendorf micropestles and incubated for 20 minutes at 37°C.

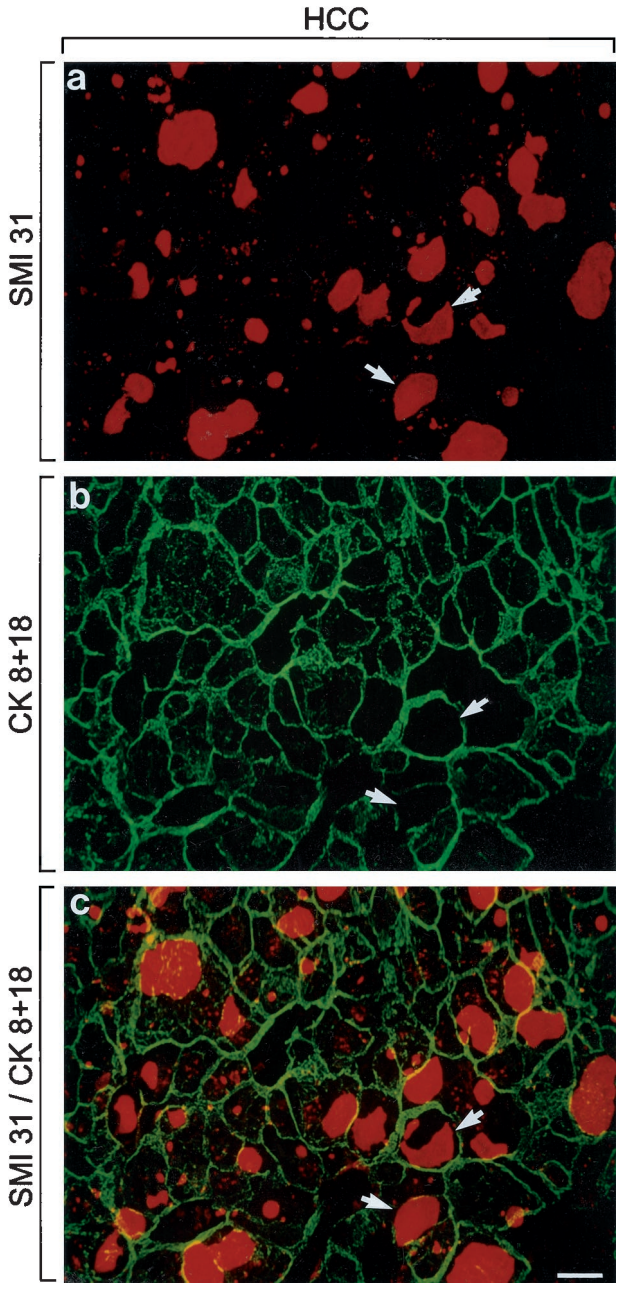

Figure 3. Single (a and b) and double (c) immunofluorescence microscopy using polyclonal antibodies to CKs 8 and 18 (b and c, green) and SMI 31 (a and c, red). Note that IHBs are strongly stained by SMI 31 but not by CK antibodies (arrows in a–c). Yellow staining results from overlap between CK filaments and IHB material at the IHB periphery. In tumor cells, the CK filament bundles are concentrated at the cell periphery. Bars, 20 μm.

Protein content was measured by the method of Bradford.[22] Isoelectric focusing was performed with nonlinear immobilized pH gradient strips ranging from pH 3.5 to 10 (Pharmacia, Uppsala, Sweden). The strips were rehydrated for at least 8 hours in rehydration solution (8 mol/L urea, 2% CHAPS, 10 mmol/L DTT, 2% v/v carrier ampholytes Resolyte, pH 3.5 to 10 (BDH, Poole, UK) and a trace of bromophenol blue) using a reswelling chamber (Pharmacia). For analytical separation (immunoblotting and silver staining), 100 μg of protein (in a volume of 70 to 100 μl) was applied on the top of the strips in sample cups. Running conditions at 15°C were as follows: voltage was increased stepwise from 300 to 500, 1000, and 1500 V during the first 80 minutes and subsequently to 3000 V to give a total of 100 kVolt-hours. After isoelectric focusing, the strips were equilibrated for 10 minutes in a solution of 0.05 mol/L TrisHCl, pH 6.8, containing 6 mol/L urea, 30% glycerol, 2% SDS, and 2% DTT, followed by a second equilibration step for 10 minutes in a solution without DTT but with 2.5% iodoacetamide and a trace of bromophenol blue. Separation in the second dimension was performed in 1.5-mm-thick SDS-polyacrylamide gradient gels (4% to 16%) in a Bio-Rad Protean II xi multi-cell (equilibrated strips were mounted on the gels with 0.5% agarose in running buffer containing 50 mmol/L Tris, 384 mmol/L glycine, 1% SDS[23]).

Proteins on analytical gels and gels after transfer were visualized by silver staining. Gels were rinsed with deionized water for 5 minutes, and proteins were fixed in ethanol/acetic acid/water (40:10:50) overnight. After washing the gels five times for 5 minutes each in deionized water they were soaked in 1% glutaraldehyde/0.5 mol/L sodium acetate for 30 minutes. This was followed by three washing steps, each for 3 minutes in deionized water, and soaking the gels twice in 0.05% 2,7-naphthalene disulfonic acid solution for 30 minutes. The gels were then washed four times for 15 minutes in deionized water and placed into the silver nitrate solution (0.8% silver nitrate, 0.3% ammoniac, 0.02 mol/L NaOH). After washing the gels in deionized water four times for 4 minutes each, they were developed in 0.005% citric acid/0.1% formaldehyde. The reaction was stopped by placing the gels into 5% Tris/2% acetic acid.

For immunoblotting, proteins were transferred electrophoretically onto nitrocellulose membranes (0.2-μm pore size; 20 mmol/L Tris, 200 mmol/L glycine, and 20% methanol as transfer buffer) in a wet blot apparatus (Bio-Rad). Thereafter, transfer membranes were blocked with 5% nonfat milk in PBS with 0.1% Tween-20 (PBS-T), followed by incubation with SMI 31 and MPM-2 or, as negative controls, with isotype-matched immunoglobulins (diluted in PBS containing 1% normal rabbit serum) overnight. After a 1-hour washing step in PBS-T, membranes were incubated with horseradish-peroxidase-conjugated rabbit anti-mouse immunoglobulins (Dako) and washed again for at least 1 hour in PBS-T. The enhanced chemiluminescence system (ECL, Amersham) was used for detection with exposure times between 5 and 60 seconds.

Sequence Analysis of the SMI 31 and MPM-2 Reactive Material

The Coomassie-blue-stained major spot of a two-dimensional gel (arrow in Fig. 5) was excised and digested in the gel with trypsin using an automated protein digestion apparatus (DigestPro, Abimed, Langenfeld, Germany). The reduction of disulfide bonds and the alkylation of cysteine residues before digestion followed the protocol recommended by Abimed. The peptides obtained were separated by high-pressure liquid chromatography (HPLC) using a Hypersil C18 BDS 3-μm LC-Packings

Table 1. Reactivity of Different Antibodies with IHBs

Positive		Negative	
(m) SMI 31	(p) Anti-α1-fetoprotein	(m) M_M 120-1	(m) Anti-neurofilament
(m) MPM-2	(p) Anti-α1-antitrypsin	(m) Anti-CK 7/8/18/19	(m) Anti-Lamin A/B_2/C
(m) RT 97	(p) Anti-α1-antichymotrypsin	(p) Anti-CK8/18	(m) Anti-MDR 1+3
(m) Anti-phosphoserine	(p) Anti-fibrinogen	(p) Anti-ubiquitin	(p) Anti-14-3-3
	(p) Anti-albumin	(m) Anti-ubiquitin	(m) Tau-1
	(p) Anti-β-amyloid	(p) Anti-αB-crystallin	(p) Anti-tau
	(m) Anti-HBs antigen	(m) Anti-HSP 60/70/90	
		(m) Anti-phosphothreonine	
		(m) Anti-phosphotyrosine	
		(m) SMI 34	

m, monoclonal mouse antibody; p, polyclonal rabbit antibody.

column (150 × 1.0 mm; BIA, Bensheim, Germany) and a 130A HPLC separation system (Applied Biosystems, Weiterstadt, Germany) with 0.1% trifluoric acid (TFA) as solvent A and 80% acetonitrile in 0.085% TFA as solvent B. The HPLC-separated fragments were sequenced on Polybrene-treated filters using a Procise 494A protein sequencer (Applied Biosystems).

Results

Microscopic Appearance of the Tumor

The majority of the tumor cells were large (larger than non-neoplastic hepatocytes) with oxyphilic cytoplasm and moderate anisokaryosis. The nuclei were enlarged and vesicular with accentuated nuclear membrane and prominent, mostly eosinophilic nucleoli. The tumor cells were arranged in trabecular and tubular (pseudoglandular) structures. Multinuclear giant cells and tumor cells with single but large and bizarre, irregular nuclei were interspersed. Most tumor cells contained oxyphilic dense hyaline inclusions varying in size from small globules, approximately half the size of the nucleus, to two to three times nuclear size, and sometimes even filling most of the cytoplasmic space (Figure 1, a and b). In the latter situation, the nucleus still occupied a central position and was almost completely surrounded by hyaline material. At their periphery, the hyaline inclusions were demarcated by a narrow clear halo. The hyaline inclusions were negative with PAS (Figure 1c) and iron (Perls) stains. With CAB they were mostly stained red and only occasionally blue (Figure 1d). The inclusions thus resembled classical IHBs.[2,4,11]

The surrounding non-neoplastic liver displayed micronodular cirrhosis with proliferated bile ductules within connective tissue septa. The liver parenchyma showed minimal steatosis and moderate siderosis. Non-neoplastic hepatocytes did not contain IHBs. MBs were not present in neoplastic and non-neoplastic hepatocytes.

Immunofluorescence Microscopy and Immunohistochemistry

IHBs strongly and homogeneously reacted with SMI 31 and MPM-2 (Figure 2, a, b, d, and e, and Figure 3, a and c) as well as with RT 97 and phosphoserine antibodies. Occasional IHBs displayed faint ubiquitin staining, but the majority of IHBs were ubiquitin negative (Figure 2, g and h). A large number of antibodies tested, including those against CKs, did not react with IHBs (Figure 3, b and c). The results are summarized in Table 1. No SMI 31, MPM-2, and RT 97 staining was revealed in non-neoplastic liver (Figure 2, a, c, d, and f).

Tumor cells, non-neoplastic hepatocytes, and bile duct epithelia reacted with CK antibodies revealing a cytoplasmic network as described previously.[15] In tumor cells the CK intermediate filament cytoskeleton network was less regular and dense than in non-neoplastic hepatocytes. CK filament bundles were displaced to the cell periphery by large IHBs (Figure 3, b and c).

Western Blotting

Homogenization of tumor and non-neoplastic peritumor liver tissue in low-salt buffer followed by centrifugation released proteins mostly ranging in molecular weights between 40 and 80 kd into the supernatant as revealed by Coomassie blue staining (Figure 4, lanes LS-S). On the basis of Coomassie blue staining, the patterns of proteins released were similar in neoplastic and non-neoplastic tissue. Treatment of the pellets with high-salt buffer extracted proteins with molecular weights between 60 and 70 kd and ~50 kd, respectively, the higher molecular weight proteins being slightly more pronounced in the tumor (Figure 4, lanes HS-S). Extraction of the resulting pellet with high-salt buffer containing Triton X-100 released a major protein with a molecular weight between 62 and 65 kd from the tumor but not from the control sample, in addition to proteins with molecular weights ~50 kd and with high molecular weight, which were retained at the interphase between stacking and resolving gels (Figure 4, lanes HSTX-S). Only minor protein bands could be electrophoretically detected in the final pellet (Figure 4, lane HSTX-P) mostly in the high molecular weight range. The differences between neoplastic and non-neoplastic tissue extracts suggest altered solubility of proteins in the neoplastic situation.

Western blotting revealed SMI 31 immunoreactive proteins exclusively in neoplastic tissue extracts. Extraction of tumor homogenates with low-salt buffer, high-salt buffer, and high-salt buffer containing Triton-X-100 released SMI 31 immunoreactive material into the supernatants (Figure 4, HCC, compare lanes LS-S, HS-S, and

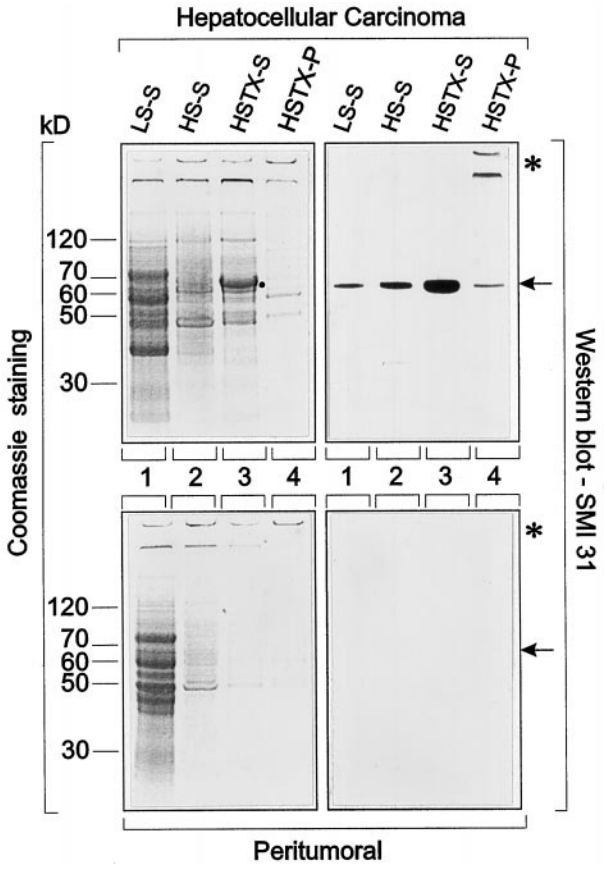

Figure 4. One-dimensional SDS-polyacrylamide gel electrophoresis and immunoblotting with SMI 31 of supernatants and pellets of homogenates of HCC (upper panel) and peritumor non-neoplastic liver (lower panel) tissue after consecutive treatment with low-salt (LS-S) and high-salt buffers without (HS-S) and with Triton X-100 (HSTX-S and HSTX-P). LS-S (lanes 1) denotes proteins in the 10,000 × *g* supernatant after homogenization of the tissues (5% w/v homogenates) in low-salt buffer. HS-S (lanes 2) denotes proteins in the 10,000 × *g* supernatant after extraction of the low-salt pellet with high-salt buffer and HSTX-S (lanes 3) denotes proteins in the 10,000 × *g* supernatant after extraction of the high-salt pellet with high-salt buffer containing Triton X-100 (Coomassie-stained gels on the left; Western blots with SMI 31 on the right side). Note that increasing amounts of the SMI 31 reactive protein (molecular weight between 62 and 65 kd; dot in Coomassie-stained gels, arrows in Western blots) are released into the supernatant derived from tumor tissue. In the final pellet of tumor material (HSTX-P; lane 4), small amounts of SMI 31 reactive proteins are left as a protein band corresponding to a molecular weight of 62 to 65 kd (arrow) and at the interphase between stacking and resolving gels and in the well (asterisk). In extracts and pellet derived from peritumor non-neoplastic liver, no 62- to 65-kd protein band is detected by immunoblotting (compare lower with upper panels).

HSTX-S). In the final sediment, some immunoreactive material with a molecular weight between 62 and 65 kd and with high molecular weights trapped in the well and at the interface between stacking and resolving gel (probably resembling aggregated protein) remained (Figure 4, lane HSTX-P). In non-neoplastic (peritumor) liver treated identically, no SMI 31 immunoreactivity was observed (Figure 4, peritumor). With MPM-2 and phosphoserine antibodies, identical results were obtained (not shown). In two-dimensional Western blots the SMI-31-immunoreactive material was resolved into several highly acidic (pH ~4.5) isoelectric variants. Similar, but not identical, immunoreactivity was observed with MPM-2 antibodies (Figure 5), suggesting that these antibodies recognize different phosphoepitopes on this protein.

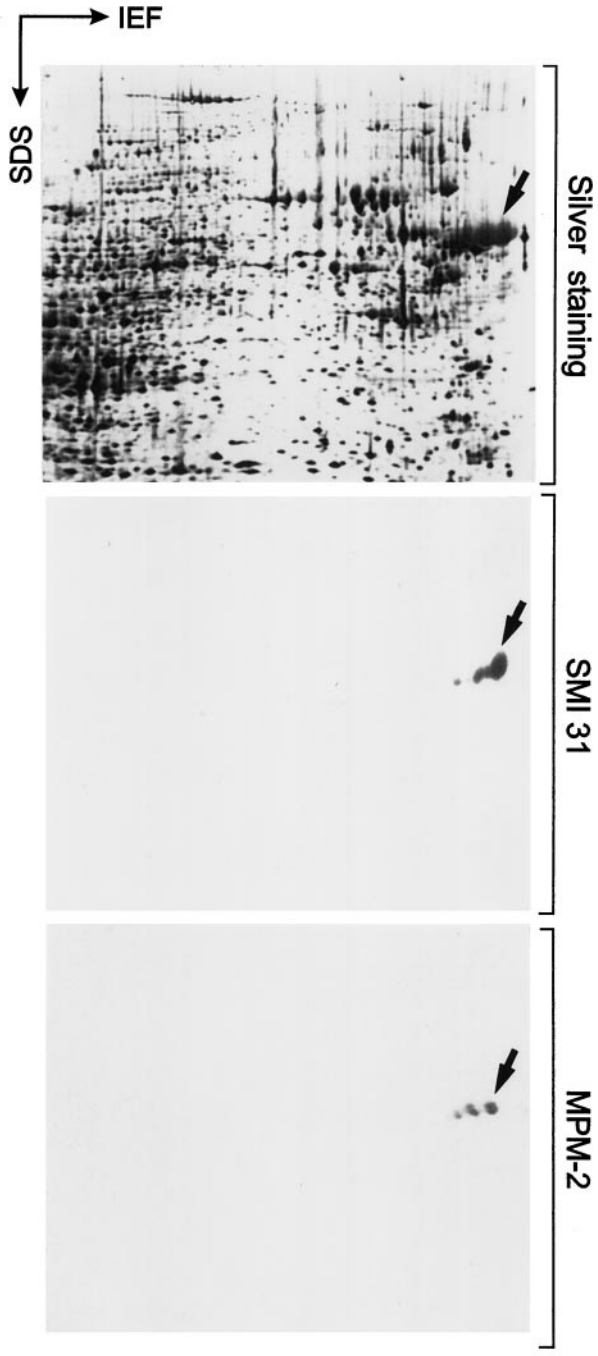

Figure 5. Immunoblots with SMI 31 and MPM-2 after two-dimensional gel electrophoresis of tumor homogenate containing IHBs. Proteins present in the homogenate are demonstrated by silver staining (upper panel). Note reactivity of SMI 31 (middle panel) and MPM-2 (lower panel) in Western blots with a set of acidic proteins corresponding to molecular weights of 62 to 65 kd and isoelectric pH values ~4.5 (arrows). These proteins resemble isoelectric variants, possibly with different degrees of phosphorylation. IEF, direction of isoelectric focusing; SDS, direction of SDS gel electrophoresis.

Electron Microscopy

IHBs displayed a heterogeneous ultrastructure. They consisted of beaded filaments with diameters of ~10 nm in irregular as well as parallel arrangement (Figure 6). Beads or granules measuring 10 nm in diameters

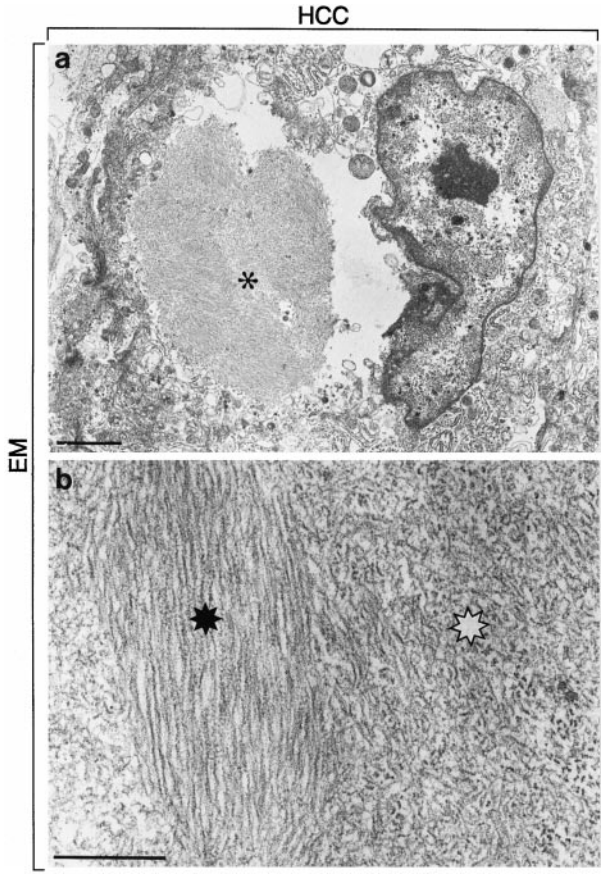

Figure 6. The electron micrograph depicts a cancer cell containing an IHB (a, asterisk). The IHB shows ultrastructural heterogeneity. It consists of parallel filaments with diameters of ~10 nm (black asterisk in b) but also of less distinct shorter beaded haphazardly arranged filaments (white asterisk in b). Bars, 2 μm (a) and 0.5 μm (b).

seemed to constitute the subunits. Although a similar ultrastructure has been described for MB filaments,[12,24,25] IHB filaments are less distinct and more granular (Figure 6, a and b) than MB filaments.

Protein Sequence Analysis of the SMI 31 and MPM-2 Immunoreactive Material

By microsequencing of HPLC peaks obtained after digestion of the major protein spot (arrow in Figure 5) three distinct amino acid sequences were obtained: 1) VAALFPALRP, 2) LAFPSPFGHL, and 3) EAALYPHLPP. Each of these peptides could be aligned to the p62 protein sequence reported by Joung et al.[18] In fact, they were completely identical with positions 51 to 60, 166 to 175, and 379 to 388 of p62 (Figure 7; Gen Bank accession U46751). Thus, the analyzed fragments corresponded to different domains located in the amino-terminal, middle, and carboxy-terminal regions of p62, indicating that the sequence identity of the IHB component is not restricted to only one part of the protein.

```
1   MASLTVKAYLLGKEDAAREIRRFSFCCSPEPEAEAEAAAG
41  PGPCERLLSR**VAALFPALRP**GGFQAHYRDEDGDLVAFSSD
81  EELTMAMSYVKDDIFRIYIKEKKECRRDHRPPCAQEAPRN
121 MVHPNVICDGCNGPVVGTRYKCSVCPDYDLCSVCEGKGLH
161 HTK**LAFPSPFGH**LSEGFSHSRWLRKVKHGHFGWPGWEM
201 GPPGNWSPRPPRAGEARPGPTAESASGPSEDPSVNFLKNV
241 GESVAAALSPLGIEVDIDVEHGGKRSRLTPVSPESSSTEE
281 KSSSQPSSCCSDPSKPGGNVEGATQSLAEQMRKIALESEG
321 PEEQMESDNCSGGDDDWTHLSSKEVDPSTGELQSLQMPE
361 SEGPSSLDPSQEGPTGLK**EAALYPHLPP**EADPRLIESLSQ
401 MLSMGFSDEGGWLTRLLQTKNYDIGAALDTQYSKHPPPL
```

Figure 7. Sequence of p62.[18] The three sequences in bold type covering the positions 51 to 60, 166 to 175, and 379 to 388 are identical to the three sequences obtained by microsequencing of the major Coomassie-blue-stained spot derived from IHB material indicated in Figure 5 (arrow). The analyzed fragments correspond to different domains located in the amino-terminal, middle, and carboxy-terminal regions of p62.

Discussion

HCC cells may contain a variety of intracytoplasmic inclusions differing in morphology and chemical composition.[1–11] However, IHBs (globular hyalin[1,2,4,5,11]) have so far evaded further characterization. The HCC case presented in this communication was exceptional as IHBs were particularly numerous in the tumor cells allowing further analysis of this material. The identification of IHB components after solubilization was facilitated by the fact that IHBs *in situ* strongly reacted with antibodies to phosphorylated protein (serine) epitopes (SMI 31, RT 97, MPM-2, and anti-phosphoserine). Immunoreactive IHB components were soluble in buffers with low and high salt concentration, and solubility was enhanced by non-ionic detergents (Triton X-100). Under these conditions most of the immunoreactive IHB material was recovered in the supernatant after centrifugation at 10,000 × *g* and corresponded to a protein with apparent molecular weight between 62 and 65 kd. It consisted of several isoelectric variants with isoelectric pH values around pH 4.5, possibly resembling different degrees of phosphorylation. Sequence analysis of peptides derived from this protein revealed identity with p62, a novel cytosolic protein that has recently been identified as a phosphotyrosine-independent ligand of the SH2 domain of $p56^{lck}$, which is a member of the c-src family of cytoplasmic tyrosine kinases found predominantly in lymphatic (T) cells.[18,19] In this context the work of Joung et al[18] suggests that p62 plays a role in the transduction of extracellular signals by linking a membrane proximal tyrosine kinase signal with a downstream Ser/Thr kinase cascade. As p62 is also a substrate for the associated Ser/Thr kinase it is likely that its activity is regulated by phosphorylation. The expression of p62 mRNA in many tissues indicates that the functions of p62 are not restricted to lymphoid cells but rather that this protein serves a more common cellular signal transduction mechanism.[18]

To the best of our knowledge, IHBs observed in the HCC presented are the first examples of a pathological accumulation of p62. Their further analysis could be useful in elucidating the function of this protein under physiological and pathological conditions. Aggregation of p62 in HCC cells could be due to alteration of p62 structure, profound disturbance of its metabolism (ie, synthesis or degradation), or modification of associated proteins. Al-

though the exact chemical composition of IHBs is still unknown, the analysis of soluble material by one- and two-dimensional gel electrophoresis and by immunoblotting using phospho-epitope antibodies suggests that p62 is a major (although probably not the only) component of IHBs and that it is phosphorylated (phosphorylation may account for the slightly higher molecular weight of IHB-associated p62 as compared with normal p62[18,19]). Although phosphorylation seems to be involved in the regulation of its function, hyperphosphorylation, on the other hand, may have adverse effects in this respect and may contribute to its accumulation. At least *in vitro*, the interaction of p62 with the $p56^{lck}$ SH2 domain is impaired in the presence of phosphatase inhibitors.[19] The serines and threonines as components of the PEST motif present in p62 are expected to be targets for several kinases, including Ser/Thr kinase but also proline-directed kinase.[19] It is noteworthy in this context that p62-containing IHBs are not ubiquitinated, in contrast to many other abnormal intracytoplasmic protein aggregates, including MBs in alcoholic hepatitis and related disorders, Lewy bodies associated with Parkinson's, and neurofibrillary tangles with Alzheimer's disease.[26,27] This was unexpected in view of the ubiquitin-binding capacity of normal p62.[28] Lack of ubiquitination could be due to abnormal composition or configuration of the ubiquitin binding (carboxy-terminal) domain of p62 in IHBs.

The reactivity of IHBs with antibodies to different phospho-epitopes not only demonstrates phosphorylation but also throws some light on the kinases involved. SMI 31 as well as MPM-2 recognize phospho-epitopes that are present on paired helical filament-associated tau in Alzheimer's disease but also on other proteins.[29–32] Despite sharing phospho-epitopes with abnormal paired helical filament-associated tau proteins, at least in its pathological state, as revealed by SMI 31 immunostaining, p62 does not seem to have a more intimate relationship to tau proteins as proved by the sequence data. MPM-2 was raised against mitotic HeLa cell extracts and has been shown to react with ~40 proteins that are synthesized during interphase and become MPM-2 reactive after entering M-phase, apparently due to the action of M-phase-specific kinases.[33,34] Particularly, *in vitro* studies suggest that $p34^{cdc2}$ but also mitogen-activated protein (MAP) kinase may be involved in the production of the MPM-2 reactive epitope. The distribution of MPM-2 antigens in a wide variety of species, including plants, indicates pronounced evolutionary conservation of mitosis-specific phosphorylation.[35] MPM-2 also recognizes one of the two regulatory phosphorylation sites on MAP kinase, a member of a family of kinases that are regulated by extracellular signals and involved in the activation of G0 and G2 arrested cells. Phosphorylation of the MPM-2 epitope leads to a decrease in MAP kinase activity *in vitro*. As MPM-2 can inhibit ubiquitin-mediated destruction of cyclin B (determined with *Xenopus* egg extracts[35]), a relationship between p62 MPM-2 immunoreactivity and function can be anticipated. In fact, the reaction of MPM-2 antibodies with p62 further supports the assumption of an important role of p62 in signal transduction, mitosis, and cell cycle regulation and the role of mitosis-related kinases in p62 phosphorylation, at least in the pathological situation of IHB formation in HCC cells.

Some authors emphasized a relationship between IHBs and MBs on the basis of light and electron microscopic similarities and their occasional simultaneous presence in HCC cells.[1,2,4] Particularly, the filamentous ultrastructure of IHBs resembles MB filaments types I and II as first described by Yokoo et al.[24] However, there are still significant differences to reject a close relation between IHBs and MBs. The major distinguishing feature is the absence of CKs, which are major constituents of MBs, in IHBs.[12,15] Moreover, the almost complete lack of ubiquitination of IHBs in contrast to MBs and other types of cytoskeleton-related inclusion bodies, such as neurofibrillary tangles in Alzheimer's disease, Lewy bodies in Parkinson's disease, neuronal inclusions in motor neuron disease (amyotrophic lateral sclerosis), and astrocytic Rosenthal fibers,[26,27] is another significant distinguishing feature. On the other hand, IHBs share SMI 31 and MPM-2 immunoreactivity with MBs[36] (C. Stumptner, A. Fuchsbichler, M. Lehner, K. Zatloukal, H. Denk, in preparation) and neurofibrillary tangles.[29–32] This suggests similarities in pathogenesis that deserve further attention. The elucidation of the mechanisms involved in IHB formation may, therefore, shed light not only on common pathogenetic mechanisms associated with cellular inclusion body formation but also on regulatory principles in neoplastic and non-neoplastic hepatocytes.

Acknowledgments

We thank Rainer Zenz for his help with two-dimensional gel electrophoresis.

References

1. Norkin SA, Campagna-Pinto D: Cytoplasmic hyaline inclusions in hepatoma. Arch Pathol 1968, 86:25–32
2. Dekker A, Krause JR: Hyaline globules in human neoplasms. Arch Pathol 1973, 95:178–181
3. Thung SN, Gerber MA, Sarno E, Popper H: Distribution of five antigens in hepatocellular carcinoma. Lab Invest 1979, 41:101–105
4. Mac Donald K, Bedard YC: Cytologic, ultrastructural and immunologic features of intracytoplasmic hyaline bodies in fine needle aspirates of hepatocellular carcinoma. Acta Cytol 1990, 34:197–200
5. Haratake J, Horie A, Setojima M: Globular cytoplasmic inclusion bodies in a metastatic hepatocellular carcinoma of the iliac bone. Ultrastruct Pathol 1990, 14:283–288
6. Nakashima O, Sugihara S, Eguchi A, Taguchi J, Watanabe J, Kojiro M: Pathomorphologic study of pale bodies in hepatocellular carcinoma. Acta Pathol Jpn 1992, 42:414–418
7. Chedid A, Chejfec G, Eichorst M, Villamil F, Terg R, Telenta M, Hojman R: Antigenic markers of hepatocellular carcinoma. Cancer 1990, 65:84–87
8. Hoso M, Nakanuma Y: Clinicopathological characteristics of hepatocellular carcinoma bearing Mallory bodies: an autopsy study. Liver 1990, 10:264–268
9. Terada T, Hoso M, Nakanuma Y: Mallory body clustering in adenomatous hyperplasia in human cirrhotic livers: report of four cases. Hum Pathol 1989, 20:886–890
10. Callea F, Favret M, Marino C, Brisigotti M: Pathology of hepatocellular carcinoma. J Surg Oncol Suppl 1993, 3:168–169

11. Anthony PP: Tumours and tumour-like lesions of the liver and biliary tract. Pathology of the Liver, ed 3. Edited by Mac Sween RNM, Anthony PP, Scheuer PJ, Burt AD, Portmann BC. Churchill Livingstone, Edinburgh, 1994, pp 635–711
12. Denk H, Franke WW, Kerjaschki D, Eckersdorfer R: Mallory bodies in experimental animals and in man. Int Rev Exp Pathol 1979, 20:77–121
13. Zatloukal K, Denk H, Spurej G, Lackinger E, Preisegger KH, Franke WW: High molecular weight component of Mallory bodies detected by a monoclonal antibody. Lab Invest 1990, 62:427–434
14. Hutter H, Zatloukal K, Winter G, Stumptner C, Denk H: Disturbance of keratin homeostasis in griseofulvin-intoxicated mouse liver. Lab Invest 1993, 69:576–582
15. Denk H, Franke WW, Dragosics B, Zeiler I: Pathology of cytoskeleton in liver cells: demonstration of Mallory bodies (alcoholic hyalin) in murine and human hepatocytes by immunofluorescence microscopy using antibodies to cytokeratin polypeptides from hepatocytes. Hepatology 1981, 1:9–20
16. Jensen K, Gluud C: The Mallory body: theories on development and pathological significance. Hepatology 1994, 20:1330–1342
17. Salmhofer H, Rainer I, Zatloukal K, Denk H: Posttranslational events involved in griseofulvin-induced keratin cytoskeleton alterations. Hepatology 1994, 20:731–740
18. Joung I, Strominger JL, Shin J: Molecular cloning of a phosphotyrosine-independent ligand of the $p56^{lck}$ SH2 domain. Proc Natl Acad Sci USA 1996, 93:5991–5995
19. Park I, Chung J, Walsh CT, Yun Y, Strominger JL, Shin J: Phosphotyrosine-independent binding of a 62-kDa protein to the src homology 2 (SH2) domain of $p56^{lck}$ and its regulation by phosphorylation of Scr-59 in the lck unique N-terminal region. Proc Natl Acad Sci USA 1995, 92:12338–12342
20. Brion JP, Couck AM, Anderton BH: Isolated PHF and PHF-tau (A68) polypeptides in Alzheimer's disease contain epitopes from the whole sequence of different tau isoforms and modified sites recognized by RT97 and 8D8 anti-neurofilament antibodies. Neurobiol Aging 1992, 18:54–55
21. Höger TH, Zatloukal K, Waizenegger I, Krohne G: Characterization of a second highly conserved B-type lamin present in cells previously thought to contain only a single B-type lamin. Chromosoma 1990, 99:379–390
22. Bradford MM: A rapid and sensitive method for the quantitation of microgram quantities of protein utilizing the principle of protein-dye binding. Anal Biochem 1976, 72:248–254
23. Pasquali C, Fialka I, Huber LA: Preparative two-dimensional gel electrophoresis of membrane proteins. Electrophoresis 1997, 18:2573–2581
24. Yokoo H, Minick OT, Batti F, Kent G: Morphologic variants of alcoholic hyalin. Am J Pathol 1972, 69:25–40
25. Wiggers KD, French SW, French BA, Carr BN: The ultrastructure of Mallory body filaments. Lab Invest 1973, 29:652–658
26. Lowe J, Blanchard A, Morell K, Lennox G, Reynolds L, Billet M, Landon M, Mayer RJ: Ubiquitin is a common factor in intermediate filament inclusion bodies of diverse type in man, including those of Parkinson's disease, Pick's disease, and Alzheimer's disease, as well as Rosenthal fibers in cerebellar astrocytomas, cytoplasmic bodies in muscle, and Mallory bodies in alcoholic liver disease. J Pathol 1988, 155:9–15
27. Lowe J, Mayer RJ, Landon M: Ubiquitin in neurodegenerative disease. Brain Pathol 1993, 3:55–65
28. Vadlamudi RK, Joung I, Strominger JL, Shin J: p62, a phosphotyrosine-independent ligand of the SH2 domain of $p56^{lck}$, belongs to a new class of ubiquitin-binding proteins. J Biol Chem 1996, 271: 20235–20237
29. Nukina N, Kosik KS, Selkoe DJ: Recognition of Alzheimer paired helical filaments by monoclonal neurofilament antibodies is due to crossreaction with tau protein. Proc Natl Acad Sci USA 1987, 84: 3415–3419
30. Lichtenberg-Kraag B, Mandelkow EM, Biernat J, Steiner B, Schröter C, Gustke N, Meyer HE, Mandelkow E: Phosphorylation-dependent epitopes of neurofilament antibodies on tau protein and relationship with Alzheimer tau. Proc Natl Acad Sci USA 1992, 89:5384–5388
31. Vincent I, Rosado M, Davies P: Mitotic mechanisms in Alzheimer's disease? J Cell Biol 1996, 132:413–425
32. Kondratick CM, Vandre DD: Alzheimer's disease neurofibrillary tangles contain mitosis-specific phosphoepitopes. J Neurochem 1996, 67:2405–2416
33. Davis FM, Isao TY, Fowler SK, Rao PN: Monoclonal antibodies to mitotic cells. Proc Natl Acad Sci USA 1983, 80:2926–2930
34. Westendorf JM, Rao PN, Gerace L: Cloning of cDNAs for M-phase phosphoproteins recognized by the MPM2 monoclonal antibody and determination of the phosphorylated epitope. Proc Natl Acad Sci USA 1994, 91:714–718
35. Renzi L, Gersch MS, Campbell MS, Wu L, Osmani SA, Gorhsky GJ: MPM-2 antibody-reactive phosphorylations can be created in detergent-extracted cells by kinetochore-bound and soluble kinases. J Cell Sci 1997, 110:2013–2025
36. Preisegger KH, Zatloukal K, Spurej G, Riegelnegg D, Denk H: Common epitopes of human and murine Mallory bodies and Lewy bodies as revealed by a neurofilament antibody. Lab Invest 1992, 66:193–199